organic compounds

Hydrogen-bonded sheet structures in neutral, anionic and hydrated 6-amino-2-(morpholin-4-yl)-5-nitroso-pyrimidines

Fabían Orozco,[a] Braulio Insuasty,[a] John N. Low,[b] Justo Cobo[c] and Christopher Glidewell[d]*

[a]Departamento de Química, Universidad de Valle, AA 25360 Cali, Colombia, [b]Department of Chemistry, University of Aberdeen, Meston Walk, Old Aberdeen AB24 3UE, Scotland, [c]Departamento de Química Inorgánica y Orgánica, Universidad de Jaén, 23071 Jaén, Spain, and [d]School of Chemistry, University of St Andrews, Fife KY16 9ST, Scotland
Correspondence e-mail: cg@st-andrews.ac.uk
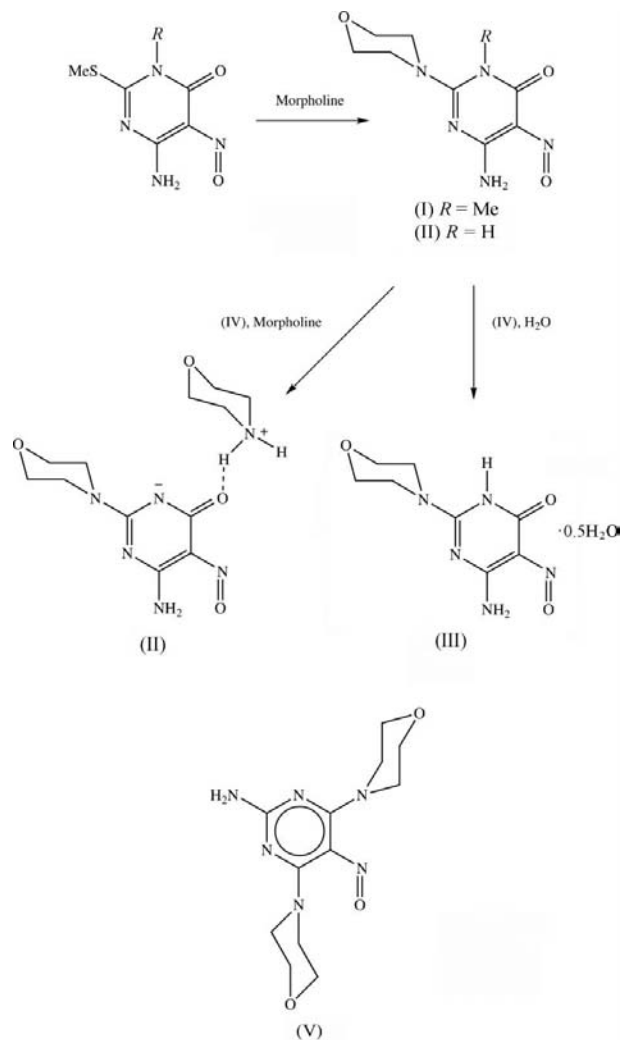
In each of 6-amino-3-methyl-2-(morpholin-4-yl)-5-nitrosopyrimidin-4(3H)-one, $C_9H_{13}N_5O_3$, (I), morpholin-4-ium 4-amino-2-(morpholin-4-yl)-5-nitroso-6-oxo-1,6-dihydropyrimidin-1-ide, $C_4H_{10}NO^+ \cdot C_8H_{10}N_5O_3^-$, (II), and 6-amino-2-(morpholin-4-yl)-5-nitrosopyrimidin-4(3H)-one hemihydrate, $C_8H_{11}N_5O_3 \cdot 0.5H_2O$, (III), the bond distances within the pyrimidine components are consistent with significant electronic polarization, which is most marked in (II) and least marked in (I). Despite the high level of substitution, the pyrimidine rings are all effectively planar, and in each of the pyrimidine components, there are intramolecular N—H···O hydrogen bonds. In each compound, the organic components are linked by multiple N—H···O hydrogen bonds to form sheets of widely differing construction, and in compound (III) adjacent sheets are linked by the water molecules, so forming a three-dimensional hydrogen-bonded framework. This study also contains the first direct geometric comparison between the electronic polarization in a neutral aminonitrosopyrimidine and that in its ring-deprotonated conjugate anion in a metal-free environment.

Comment

Substituted 6-amino-5-nitrosopyrimidines often form intramolecular N—H···O hydrogen bonds and hence they are isoelectronic and approximately isosteric with the correspondingly substituted purines. The presence of the 5-nitroso substituent strongly activates nucleophilic displacement of 2-methoxy or 2-methylsulfanyl substituents and this has provided an effective and versatile synthetic route to a wide range of 2-substituted derivatives (Melguizo *et al.*, 2002). The use of 2-methylsulfanyl derivatives as substrates is particularly

attractive as the low boiling temperature of the methanethiol by-product (*ca* 279 K at normal pressure) means that this component is readily removed as the reaction proceeds, so driving the substitution to completion.

Thus, reaction of 6-amino-3-methyl-2-methylsulfanyl-5-nitrosopyrimidin-4(3H)-one with morpholine gave 6-amino-3-methyl-2-(morpholin-4-yl)-5-nitrosopyrimidin-4(3H)-one, (I) (see reaction scheme above), while a similar reaction using 6-amino-2-methylsulfanyl-5-nitrosopyrimidin-4(3H)-one provided 6-amino-2-(morpholin-4-yl)-5-nitrosopyrimidin-4(3H)-one, (IV); recrystallization of (IV) from water gave the hemihydrate (III), while crystallization in the presence of morpholine gave the salt morpholin-4-ium 4-amino-2-(morpholin-4-yl)-5-nitroso-6-oxo-1,6-dihydropyrimidin-1-ide, (II). Accordingly, we have been able to compare the intramolecular metrics of both the neutral pyrimidinone (IV), as it occurs in hemihydrate (III), and the corresponding conjugate anion, as it occurs in salt (II).

While the morpholine rings in compounds (I)–(III) (Figs. 1–3) all adopt chair conformations, the pyrimidine rings are, in every case, effectively planar; the maximum deviation from the mean ring planes is 0.033 (2) Å for atom N3 in (I), 0.033 (2) Å for C4 and C5 in (II), and 0.028 (3) Å for N3 in
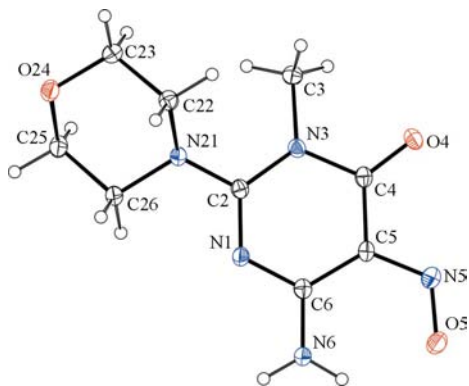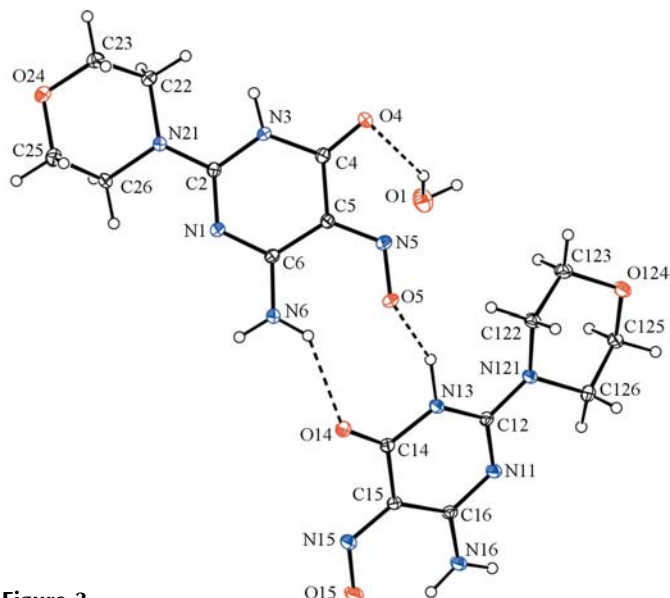
Figure 1
The molecule of compound (I), showing the atom-labelling scheme. Displacement ellipsoids are drawn at the 30% probability level and, for the sake of clarity, the intramolecular N—H···O hydrogen bond has been omitted.

(III). This may be contrasted with the boat conformation found for the pyrimidine ring in the related compound 2-amino-4,6-bis(morpholin-4-yl)-5-nitrosopyrimidine, (V) (Quesada *et al.*, 2004), and the boat (Trilleras *et al.*, 2008) and twist-boat (Quesada *et al.*, 2002, 2003; Melguizo *et al.*, 2003) conformations found in a number of other heavily substituted pyrimidines. In compounds (I)–(III), the three adjacent substituents at positions 4, 5 and 6 are of low steric bulk and the planarity of the pyrimidine rings in these examples is consistent with our earlier suggestion that the ring puckering in substituted pyrimidines is a direct consequence of steric clashes between bulky substituents in these adjacent positions (Melguizo *et al.*, 2003). The orientation of the nitroso substituents, which are all effectively coplanar with the adjacent pyrimidine rings allowing the formation of intramolecular N—H···O hydrogen bonds (Tables 1–3), are almost certainly controlled by the electronic structures discussed below.

The pyrimidine components of compounds (I)–(III) show a number of values (Table 4) which are atypical of their general types (Allen *et al.*, 1987), but which are typical of those commonly observed in related aminonitrosopyrimidines (Low *et al.*, 2000, 2001; Melguizo *et al.*, 2003; Quesada *et al.*, 2002, 2004). The discussion of these distances and their significance is based, to a large extent, on our earlier analysis (Low *et al.*, 2000) of the molecular structures of some nitrosopyrimidinyl derivatives of amino acids, where the analysis of the experimental structures was supported by database and molecular-modelling studies. This analysis showed that the difference between the C—N and N—O bond distances, conveniently denoted as Δ, provides a powerful diagnostic tool for the identification of polarized molecular–electronic structures in such compounds. In simple C-substituted nitroso compounds where there is no possibility of significant electronic delocalization, the difference between the C—N and N—O bond distances usually exceeds 0.20 Å (Talberg, 1977; Schlemper *et al.*, 1986), while the N—O distances rarely exceed 1.25 Å (Davis *et al.*, 1965; Bauer & Andreassen, 1972; Talberg, 1977; Schlemper *et al.*, 1986). However, in each of compounds (I)–(III), the value of Δ is significantly less than 0.10 Å, while the N—O distances always exceed 1.27 Å (Table 4), and the
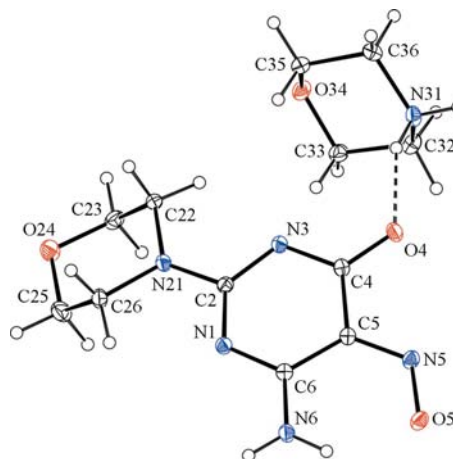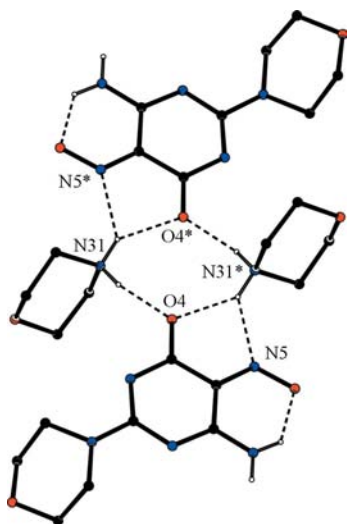

Figure 2
The independent ionic components of compound (II), showing the atom-labelling scheme and the N—H···O hydrogen bond (dashed line) linking the ions. Displacement ellipsoids are drawn at the 30% probability level and, for the sake of clarity, the intramolecular N—H···O hydrogen bond in the anion has been omitted.

Figure 3
The independent molecular components of compound (III), showing the atom-labelling scheme and the hydrogen bonds (dashed lines) linking the components. Displacement ellipsoids are drawn at the 30% probability level and, for the sake of clarity, the intramolecular N—H···O hydrogen bonds have been omitted.
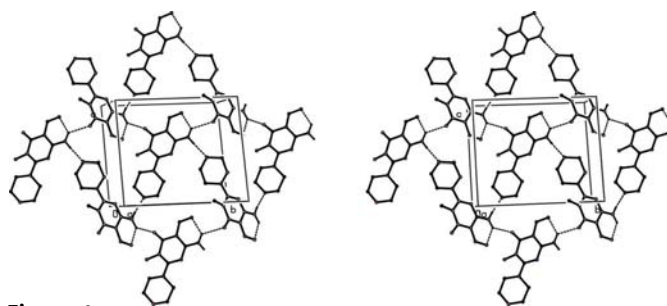
Figure 4
A stereoview of part of the crystal structure of compound (I), showing the formation of a hydrogen-bonded sheet of $S(6)$ and $R_4^4(26)$ rings parallel to (100). For the sake of clarity, H atoms bonded to C atoms have been omitted.
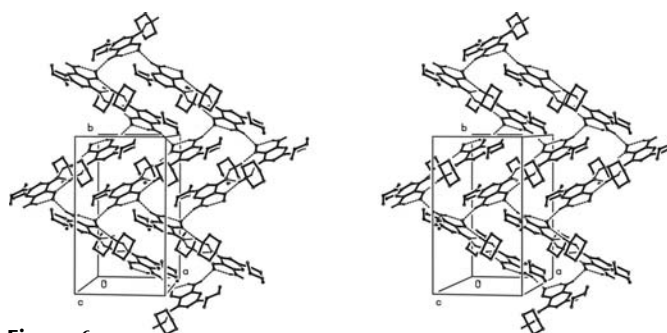
Figure 5
Part of the crystal structure of compound (II), showing the formation of a centrosymmetric aggregate of two cations and two anions. Atoms marked with an asterisk (*) are at the symmetry position $(\frac{3}{2} - x, \frac{3}{2} - y, \frac{1}{2} - z)$. For the sake of clarity, H atoms bonded to C atoms and the unit-cell outline have been omitted.

observed values here can be taken as diagnostic of significant electronic delocalization (Low *et al.*, 2000).

In the neutral compound (I), where the polarization is least marked, as judged by the magnitude of Δ, the C6—N6 bond is short for its type (Allen *et al.*, 1987), while the C2—N21 bond distance is fairly typical of its type; in addition, the C4—C5 and C5—C6 distances have very similar lengths, although in the classical representation of (I), these are formally single and double bonds, respectively; on the other hand, the N1—C2 bond, which is formally a double bond, is significantly shorter than any other C—N bond within the ring. These observations taken together point to the polarized form (I*a*) (see scheme below) as an important contributor to the overall molecular–electronic structure, in addition to the classical unpolarized form (I).
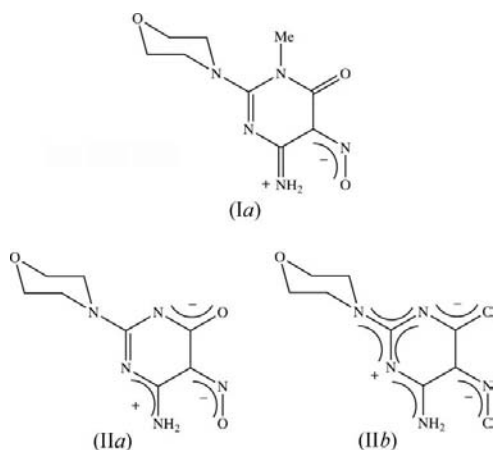
The anionic component of salt (II) shows the most marked polarization, as indicated by the very small value of Δ. In addition, the C6—N1 and C6—N6 bonds have effectively identical lengths and the C—O bond is long for its type, while the N3—C4 bond is much shorter in (II) than in (I). The
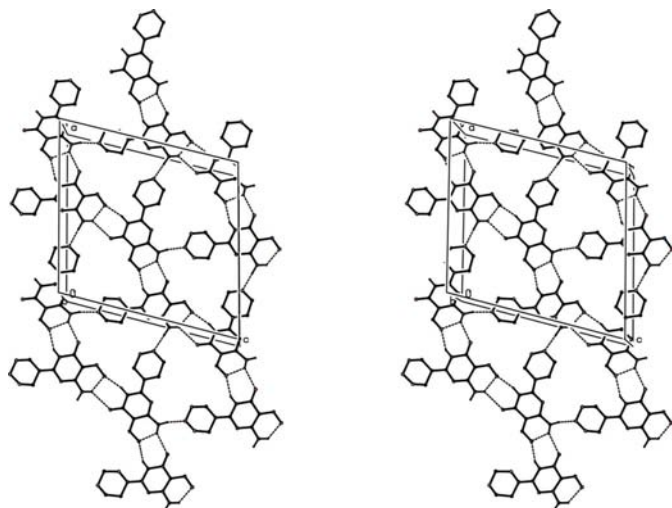

Figure 6
A stereoview of part of the crystal structure of compound (II), showing the formation of a hydrogen-bonded sheet parallel to (001) and containing four independent types of ring. For the sake of clarity, H atoms bonded to C atoms have been omitted.

combination of these observations points to the importance of the polarized form (II*a*) (see scheme above) as a contributor to the overall molecular–electronic structure. The additional observation that the C2—N1, C2—N3 and C2—N21 bonds have lengths which are identical within experimental uncertainty suggests that form (II*b*), where the positive charge is delocalized over four N-atom centres (N1, N3, N6 and N21) in an aminomethyleneguanidinium fragment, may also be significant.

In compound (III), the dimensions of the two independent pyrimidine components are very similar. The values of Δ are intermediate between those in compounds (I) and (II), but the general pattern in the intermolecular distances resembles that in (I). Thus, the C*x*4—C*x*5 and C*x*5—C*x*6 distances (*x* = nil or 1) are identical, the C*x*6—N*x*6 distances do not differ from the corresponding distance in (I), and the C—O distances are normal, although the N*x*3—C*x*4 distances are somewhat shorter than the N3—C4 distance in (I), whereas a modest lengthening might have been expected. A polarized structure of the same type as (I*a*) is indicated, but with the degree of polarization somewhat enhanced over that in compound (I).

For each of compounds (I)–(III), the supramolecular aggregation is dominated by the formation of hydrogen-bonded sheets. In (I), the sheet is built from just three hydrogen bonds, all of N—H⋯O type (Table 1). Amino atom N6 in the molecule at (*x*, *y*, *z*) acts as hydrogen-bond donor, *via* H6*A* and H6*B*, respectively, to morpholine atom O24 in the molecule at $(\frac{3}{2} - x, \frac{1}{2} + y, \frac{1}{2} - z)$ and ketonic atom O4 in molecule at $(\frac{3}{2} - x, \frac{1}{2} + y, \frac{3}{2} - z)$; the latter of these is, in fact, the longer component of a planar three-centre N—H⋯(O)$_2$ system (Table 1). These intermolecular interactions, acting independently, generate $C(9)$ and $C(6)$ chains, respectively, both running parallel to the [010] direction, and in combination they generate a sheet lying parallel to (100) containing equal numbers of $S(6)$ and $R_4^4(26)$ (Bernstein *et al.*, 1995) rings (Fig. 4). Two sheets of this type, occupying the domains $0 < x < \frac{1}{2}$ and $\frac{1}{2} < x < 1$, respectively, and related to one another by inversion, pass through each unit cell, but there are no direction-specific interactions between adjacent sheets.

The formation of the sheet structure of compound (II) is somewhat more complex than that in compound (I); not only are there two independent molecular species present, but the
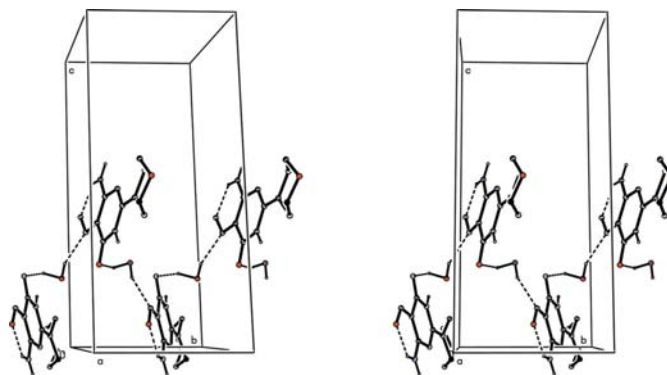
Figure 7
A stereoview of part of the crystal structure of compound (III), showing the formation of a hydrogen-bonded sheet parallel to (010) and containing five independent types of ring. For the sake of clarity, H atoms bonded to C atoms have been omitted.

Figure 8
A stereoview of part of the crystal structure of compound (III), showing the formation of a hydrogen-bonded $C_2^2(7)$ chain along [010] linking the sheets parallel to (010). For the sake of clarity, H atoms bonded to C atoms have been omitted.

number of hydrogen bonds (Table 2) is also greater. However, the sheet formation is quite easily analyzed in terms of a centrosymmetric aggregate containing two ions of each type (Fig. 5). Within the asymmetric unit, ammonium atom N31 acts as hydrogen-bond donor, *via* H31*B*, to atom O4 in the anion. The same atom N31 in the cation at (x, y, z) also acts as hydrogen-bond donor, *via* H31*A*, to atoms O4 and N5 in the anion at $(\frac{3}{2} - x, \frac{3}{2} - y, \frac{1}{2} - z)$, in an effectively planar three-centre N—H$\cdots$(N,O) system. The resulting centrosymmetric aggregate (Fig. 5), which is centred at $(\frac{3}{4}, \frac{3}{4}, \frac{1}{4})$, contains a central $R_4^2(8)$ ring along with two symmetry-related $R_1^2(5)$ rings and two $S(6)$ rings. In the final hydrogen bond, atom N6 in the anion at (x, y, z) acts as donor to atom O4 in the anion at $(-\frac{1}{2} + x, 1 - y, z)$, and by this means the aggregate centred at $(\frac{3}{4}, \frac{3}{4}, \frac{1}{4})$ is directly linked to those at $(\frac{1}{4}, \frac{1}{4}, \frac{1}{4})$, $(\frac{1}{4}, \frac{5}{4}, \frac{1}{4})$, $(\frac{5}{4}, \frac{1}{4}, \frac{1}{4})$ and $(\frac{5}{4}, \frac{5}{4}, \frac{1}{4})$, so forming a sheet parallel to (001). This sheet thus contains four types of ring, *viz.* $S(6)$, $R_1^2(5)$, $R_4^2(8)$ and $R_8^8(30)$, the last two of which are both centrosymmetric (Fig. 6). Two sheets of this type, occupying the domains $0 < z < \frac{1}{2}$ and $\frac{1}{2} < z < 1$, respectively, and related to one another by inversion, pass through each unit cell, but there are no direction-specific interactions between adjacent sheets.

There are three independent molecular components, all neutral, in compound (III), and they are linked by a large number of hydrogen bonds, encompassing O—H$\cdots$O, O—H$\cdots$N and N—H$\cdots$O types (Table 3), into a three-dimensional framework. The two organic components are linked into sheets built from six independent intermolecular N—H$\cdots$O hydrogen bonds, and these sheets are linked by the water molecules to form the three-dimensional structure.

Within the asymmetric unit, atoms N6 and N13 act as hydrogen-bond donors to O14 and O5, respectively (Fig. 3). Similarly, atoms N16 and N3 act as donors, respectively, to O4 at $(-\frac{1}{2} + x, \frac{1}{2} - y, \frac{1}{2} + z)$ and O155 at $(\frac{1}{2} + x, \frac{1}{2} - y, -\frac{1}{2} + z)$. This combination of four hydrogen bonds thus generates a chain of

rings running parallel to the $[10\bar{1}]$ direction and built from molecules related by the *n*-glide plane at $y = \frac{1}{4}$ (Fig. 7). In addition, atom N6 at (x, y, z) acts as donor to morpholine atom O124 at $(\frac{1}{2} + x, \frac{1}{2} - y, \frac{1}{2} + z)$, so generating a second chain of rings, this time running parallel to the [101] direction, but again built from molecules related by the *n*-glide plane at $y = \frac{1}{4}$, while atom N16 at (x, y, z) acts as donor to morpholine atom O24 at $(-1 + x, y, z)$, so generating by translation a third chain of rings, this time running parallel to the [100] direction. The combination of the chains along [100], [101] and $[10\bar{1}]$ then generates a sheet parallel to (010) and containing five independent types of ring, two each of the $S(6)$ and $R_2^2(6)$ types, together with one type of $R_4^4(24)$ ring (Fig. 7).

Two such sheets, occupying the domains $0 < y < \frac{1}{2}$ and $\frac{1}{2} < y < 1$, respectively, and related to one another by inversion, pass through each unit cell, and adjacent sheets are linked by the water molecules. A combination of O—H$\cdots$O and O—H$\cdots$N hydrogen bonds forms a $C_2^2(7)$ chain running parallel to the [010] direction (Fig. 8), which links the sheets into a continuous three-dimensional structure.

In summary, compounds (I)–(III) all show polarized molecular–electronic structures, albeit in differing degrees, and the organic fragments in each compound are linked by hydrogen bonds into sheets of markedly different types, despite the rather small differences in molecular constitution between the pyrimidine fragments involved.

Experimental

For the synthesis of compound (I), morpholine (100 mmol) was added dropwise and with magnetic stirring to a suspension of 6-amino-3-methyl-2-methylsulfanyl-5-nitrosopyrimidin-4(3*H*)-one (26.8 mmol) in dry ethanol (80 ml). Stirring was continued for 18 h, when the colour changed from blue to violet as methanethiol was liberated. The resulting solid was collected by filtration and washed with cold ethanol. Crystals of (I) suitable for single-crystal X-ray diffraction were grown by slow evaporation of a solution in dimethylformamide–ethanol (10:1 *v/v*). Yield 57%; m.p. 508–509 K; MS (30 eV) *m/z* (%): 239 (M^+, 89), 209 (2), 181 (6), 153 (4), 139 (10), 125 (20), 113 (13), 109 (13), 86 (29), 69 (92), 57 (76), 42 (100). A similar reaction, but using 6-amino-2-methylsulfanyl-5-nitrosopy-

organic compounds

rimidin-4(3H)-one in place of the 3-methyl analogue gave 6-amino-2-(morpholin-4-yl)-5-nitrosopyrimidin-4(3H)-one, (IV). Yield 99%, m.p. 507–508 K; MS (30 eV) m/z (%): 225 (M^+, 72), 208 (94), 195 (2), 139 (2), 113 (49), 113 (49), 95 (24), 86 (21), 69 (100). Recrystallization of this material from a dimethylformamide–ethanol (10:1 v/v) mixture containing a little morpholine gave crystals of compound (II) suitable for single-crystal X-ray diffraction, whereas crystallization from water yielded hemihydrate (III).

Compound (I)

Crystal data

$C_9H_{13}N_5O_3$	$V = 1063.68\ (10)$ Å^3
$M_r = 239.24$	$Z = 4$
Monoclinic, $P2_1/n$	Mo $K\alpha$ radiation
$a = 8.9122\ (6)$ Å	$\mu = 0.12$ mm^{-1}
$b = 11.9051\ (7)$ Å	$T = 120\ (2)$ K
$c = 10.4111\ (4)$ Å	$0.41 \times 0.28 \times 0.25$ mm
$\beta = 105.649\ (3)°$	

Data collection

Bruker–Nonius KappaCCD diffractometer	25676 measured reflections
Absorption correction: multi-scan ($SADABS$; Sheldrick, 2003)	2445 independent reflections
	1516 reflections with $I > 2\sigma(I)$
$T_{min} = 0.959$, $T_{max} = 0.972$	$R_{int} = 0.068$

Refinement

$R[F^2 > 2\sigma(F^2)] = 0.054$	155 parameters
$wR(F^2) = 0.159$	H-atom parameters constrained
$S = 1.06$	$\Delta\rho_{max} = 0.33$ e Å^{-3}
2445 reflections	$\Delta\rho_{min} = -0.31$ e Å^{-3}

Compound (II)

Crystal data

$C_4H_{10}NO^+ \cdot C_8H_{10}N_5O_3^-$	$V = 2901.3\ (11)$ Å^3
$M_r = 312.34$	$Z = 8$
Monoclinic, $I2/a$	Mo $K\alpha$ radiation
$a = 9.4410\ (11)$ Å	$\mu = 0.11$ mm^{-1}
$b = 16.347\ (4)$ Å	$T = 120\ (2)$ K
$c = 18.799\ (5)$ Å	$0.26 \times 0.10 \times 0.10$ mm
$\beta = 90.045\ (15)°$	

Table 1
Hydrogen-bond geometry (Å, °) for (I).

D—H⋯A	D—H	H⋯A	D⋯A	D—H⋯A
N6—H6A⋯O24^i	0.88	1.98	2.848 (3)	168
N6—H6B⋯O5	0.88	1.98	2.619 (3)	129
N6—H6B⋯O4^{ii}	0.88	2.35	2.896 (3)	121

Symmetry codes: (i) $-x + \frac{3}{2}, y + \frac{1}{2}, -z + \frac{1}{2}$; (ii) $-x + \frac{3}{2}, y + \frac{1}{2}, -z + \frac{3}{2}$.

Table 2
Hydrogen-bond geometry (Å, °) for (II).

D—H⋯A	D—H	H⋯A	D⋯A	D—H⋯A
N6—H6A⋯O5^i	0.88	2.02	2.872 (2)	163
N6—H6B⋯O5	0.88	1.95	2.608 (2)	130
N31—H31A⋯O4^{ii}	0.92	2.08	2.868 (2)	143
N31—H31A⋯N5^{ii}	0.92	2.21	2.939 (2)	136
N31—H31B⋯O4	0.92	1.85	2.711 (2)	154

Symmetry codes: (i) $x - \frac{1}{2}, -y + 1, z$; (ii) $-x + \frac{3}{2}, -y + \frac{3}{2}, -z + \frac{1}{2}$.

Table 3
Hydrogen-bond geometry (Å, °) for (III).

D—H⋯A	D—H	H⋯A	D⋯A	D—H⋯A
O1—H1A⋯N5^i	0.89	2.08	2.916 (3)	157
O1—H1B⋯O4	1.19	2.37	3.423 (3)	146
N3—H3⋯O15^{ii}	0.88	2.04	2.882 (3)	161
N6—H6A⋯O124^{iii}	0.88	1.97	2.835 (3)	166
N6—H6B⋯O5	0.88	1.98	2.623 (3)	129
N6—H6B⋯O14	0.88	2.24	2.943 (3)	137
N13—H13⋯O5	0.88	2.03	2.838 (3)	152
N16—H16A⋯O24^{iv}	0.88	2.00	2.875 (3)	173
N16—H16B⋯O15	0.88	1.96	2.605 (3)	129
N16—H16B⋯O4^v	0.88	2.49	3.176 (3)	136

Symmetry codes: (i) $-x + \frac{1}{2}, y + \frac{1}{2}, -z + \frac{1}{2}$; (ii) $x + \frac{1}{2}, -y + \frac{1}{2}, z - \frac{1}{2}$; (iii) $x + \frac{1}{2}, -y + \frac{1}{2}, z + \frac{1}{2}$; (iv) $x - 1, y, z$; (v) $x - \frac{1}{2}, -y + \frac{1}{2}, z + \frac{1}{2}$.

Data collection

Bruker–Nonius KappaCCD diffractometer	33473 measured reflections
Absorption correction: multi-scan ($SADABS$; Sheldrick, 2003)	3354 independent reflections
	2361 reflections with $I > 2\sigma(I)$
$T_{min} = 0.977$, $T_{max} = 0.989$	$R_{int} = 0.048$

Refinement

$R[F^2 > 2\sigma(F^2)] = 0.049$	199 parameters
$wR(F^2) = 0.109$	H-atom parameters constrained
$S = 1.09$	$\Delta\rho_{max} = 0.25$ e Å^{-3}
3354 reflections	$\Delta\rho_{min} = -0.27$ e Å^{-3}

Compound (III)

Crystal data

$C_8H_{11}N_5O_3 \cdot 0.5H_2O$	$V = 2012.4\ (6)$ Å^3
$M_r = 234.23$	$Z = 8$
Monoclinic, $P2_1/n$	Mo $K\alpha$ radiation
$a = 16.421\ (2)$ Å	$\mu = 0.12$ mm^{-1}
$b = 7.3671\ (12)$ Å	$T = 120\ (2)$ K
$c = 17.205\ (4)$ Å	$0.44 \times 0.34 \times 0.21$ mm
$\beta = 104.794\ (12)°$	

Data collection

Bruker–Nonius KappaCCD diffractometer	47024 measured reflections
Absorption correction: multi-scan ($SADABS$; Sheldrick, 2003)	4646 independent reflections
	2535 reflections with $I > 2\sigma(I)$
$T_{min} = 0.953$, $T_{max} = 0.975$	$R_{int} = 0.098$

Refinement

$R[F^2 > 2\sigma(F^2)] = 0.058$	298 parameters
$wR(F^2) = 0.162$	H-atom parameters constrained
$S = 1.05$	$\Delta\rho_{max} = 0.32$ e Å^{-3}
4646 reflections	$\Delta\rho_{min} = -0.41$ e Å^{-3}

For each of (I) and (III), the space group $P2_1/n$ was uniquely assigned from the systematic absences. For compound (II), the systematic absences permitted Cc and $C2/c$ as possible space groups; $C2/c$ was selected and confirmed by the structure solution, but the setting was then transformed to the alternative $I2/a$. All H atoms were located in difference maps and treated as riding atoms. H atoms bonded to C or N atoms were allowed to ride in geometrically idealized positions, with C—H = 0.98 (CH$_3$) or 0.99 Å (CH$_2$) and N—H = 0.92 Å for the cation in (II) and 0.88 Å otherwise, and with U_{iso}(H) = kU_{eq}(C,N), where k = 1.5 for methyl groups and 1.2 otherwise. H atoms bonded to O atoms were permitted to ride at the locations deduced from the difference maps, with U_{iso}(H) = $1.5U_{eq}$(O), giving O—H = 0.89 and 1.19 Å in compound (III).

Table 4
Selected bond distances and angles (Å, °) for compounds (I)–(III).

Parameter	(I) x = nil	(II) x = nil	(III), mol 1 x = nil	(III), mol 2 x = 1
Nx1—Cx2	1.315 (3)	1.353 (2)	1.323 (3)	1.327 (3)
Cx2—Nx3	1.376 (3)	1.353 (2)	1.370 (3)	1.368 (3)
Nx3—Cx4	1.415 (3)	1.346 (2)	1.384 (3)	1.397 (3)
Cx4—Cx5	1.447 (3)	1.472 (3)	1.451 (4)	1.452 (4)
Cx5—Cx6	1.435 (3)	1.450 (2)	1.455 (4)	1.451 (4)
Cx6—Nx1	1.357 (3)	1.331 (2)	1.344 (3)	1.339 (3)
Cx2—Nx21	1.358 (3)	1.352 (2)	1.330 (3)	1.346 (3)
Cx4—Ox4	1.221 (3)	1.260 (2)	1.225 (3)	1.222 (3)
Cx5—Nx5	1.358 (3)	1.327 (2)	1.337 (3)	1.341 (3)
Nx5—Ox5	1.275 (3)	1.307 (2)	1.284 (3)	1.286 (3)
Cx6—Nx6	1.316 (3)	1.328 (2)	1.317 (3)	1.318 (3)
Δ^a	0.083 (3)	0.020 (2)	0.053 (3)	0.055 (3)
Cx6—Cx5—Nx5—Ox5	0.0 (3)	−2.3 (3)	−1.6 (4)	0.2 (4)

Notes: (a) Δ is the bond-length difference $[d(Cx5—Nx5) − d(Nx5—Ox5)]$.

For all compounds, data collection: *COLLECT* (Hooft, 1999); cell refinement: *DIRAX/LSQ* (Duisenberg *et al.*, 2000); data reduction: *EVALCCD* (Duisenberg *et al.*, 2003); structure solution: *SIR2004* (Burla *et al.*, 2005); structure refinement: *OSCAIL* (McArdle, 2003) and *SHELXL97* (Sheldrick, 2008); molecular graphics: *PLATON* (Spek, 2003); software used to prepare material for publication: *SHELXL97* and *PRPKAPPA* (Ferguson, 1999).

References

Allen, F. H., Kennard, O., Watson, D. G., Brammer, L., Orpen, A. G. & Taylor, R. (1987). *J. Chem. Soc. Perkin Trans. 2*, pp. S1–19.
Bauer, S. H. & Andreassen, A. L. (1972). *J. Phys. Chem.* **76**, 3099–3108.
Bernstein, J., Davis, R. E., Shimoni, L. & Chang, N.-L. (1995). *Agnew. Chem. Int. Ed. Engl.* **34**, 1555–1573.
Burla, M. C., Caliandro, R., Camalli, M., Carrozzini, B., Cascarano, G. L., De Caro, L., Giacovazzo, C., Polidori, G. & Spagna, R. (2005). *J. Appl. Cryst.* **38**, 381–388.
Davis, M. I., Boggs, J. E., Coffey, D. & Hanson, H. P. (1965). *J. Phys. Chem.* **69**, 3727–3730.
Duisenberg, A. J. M., Hooft, R. W. W., Schreurs, A. M. M. & Kroon, J. (2000). *J. Appl. Cryst.* **33**, 893–898.
Duisenberg, A. J. M., Kroon-Batenburg, L. M. J. & Schreurs, A. M. M. (2003). *J. Appl. Cryst.* **36**, 220–229.
Ferguson, G. (1999). *PRPKAPPA*. University of Guelph, Canada.
Hooft, R. W. W. (1999). *COLLECT*. Nonius BV, Delft, The Netherlands.
Low, J. N., López, M. D., Arranz Mascarós, P., Cobo Domingo, J., Godino, M. L., López Garzón, R., Gutiérrez, M. D., Melguizo, M., Ferguson, G. & Glidewell, C. (2000). *Acta Cryst.* B**56**, 882–892.
Low, J. N., Moreno Sánchez, J. M., Arranz Mascarós, P., Godino Salido, M. L., López Garzon, R., Cobo Domingo, J. & Glidewell, C. (2001). *Acta Cryst.* B**57**, 317–328.
McArdle, P. (2003). *OSCAIL for Windows*. Version 10. Crystallography Centre, Chemistry Department, NUI Galway, Ireland.
Melguizo, M., Marchal, A., Nogueras, M., Sánchez, A. & Low, J. N. (2002). *J. Heterocycl. Chem.* **39**, 97–103.
Melguizo, M., Quesada, A., Low, J. N. & Glidewell, C. (2003). *Acta Cryst.* B**59**, 263–276.
Quesada, A., Marchal, A., Low, J. N. & Glidewell, C. (2003). *Acta Cryst.* C**59**, o102–o104.
Quesada, A., Marchal, A., Melguizo, M., Low, J. N. & Glidewell, C. (2004). *Acta Cryst.* B**60**, 76–89.
Quesada, A., Marchal, A., Melguizo, M., Nogueras, M., Sánchez, A., Low, J. N., Cannon, D., Farrell, D. M. M. & Glidewell, C. (2002). *Acta Cryst.* B**58**, 300–315.
Schlemper, E. O., Murmann, R. K. & Hussain, M. S. (1986). *Acta Cryst.* C**42**, 1739–1743.
Sheldrick, G. M. (2003). *SADABS*. Version 2.10. University of Göttingen, Germany.
Sheldrick, G. M. (2008). *Acta Cryst.* A**64**, 112–122.
Spek, A. L. (2003). *J. Appl. Cryst.* **36**, 7–13.
Talberg, H. J. (1977). *Acta Chem. Scand. Ser. A*, **31**, 485–491.
Trilleras, J., Low, J. N., Cobo, J., Marchal, A. & Glidewell, C. (2008). *Acta Cryst.* C**64**, o145–o148.